ACS Catalysis

Research Article

pubs.acs.org/acscatalysis

Hydroamination of C–C Multiple Bonds with Hydrazine Catalyzed by N-Heterocyclic Carbene–Gold(I) Complexes: Substrate and Ligand Effects

Almudena Couce-Rios, Gábor Kovács, Gregori Ujaque,* and Agustí Lledós*

Departament de Química, Universitat Autònoma de Barcelona, 08193 Cerdanyola del Vallès, Spain

Supporting Information

ABSTRACT: In this work, we computationally address, from DFT calculations, mechanistic issues of the recently described hydroamination reactions catalyzed by (carbene) gold(I) complexes that use hydrazine as N-nucleophile. We have explored the hydrohydrazination of alkynes, alkenes, and allenes using three gold–carbene catalysts reported by Bertrand's and Hashmi's groups. Aspects such as the associative or dissociative nature of the ligand exchange between hydrazine and the substrate, the generation of the catalytically active π-complex, the inner- or outer-sphere mechanism for the nucleophilic attack, the nitrogen to carbon proton transfer or the relative importance of the ligand substitution, the nucleophile addition, and the proton transfer barriers in the catalytic cycle are analyzed in light of the DFT results, taking into account the nature of the carbene ligand and the substrate. The study can provide background for the design of further hydroamination reactions using simple small N-nucleophiles.

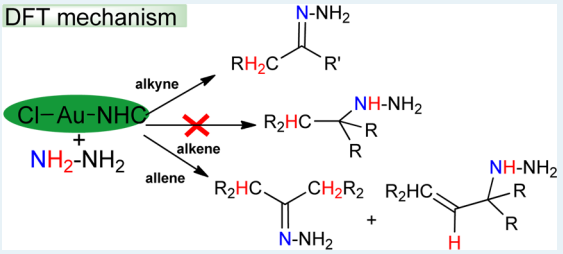

KEYWORDS: *DFT calculations, gold catalysis, hydrazine, hydroamination, N-heterocyclic carbene ligands*

INTRODUCTION

Nitrogen-containing organic compounds (either acyclic or heterocyclic) are important chemical substances, ranging from agrochemicals to pharmaceuticals. Since traditional reactions for C–N bond formation face serious limitations, hydroamination catalyzed by different transition metal homogeneous complexes have been used as an effective synthetic method for such purpose.[1−8] Several late transition metal complexes were found to be active catalysts of hydroamination reactions.[9] Previously, these homogeneous catalysts had palladium,[10−12] rhodium,[13−15] ruthenium,[16,17] and platinum[18,19] centers. In recent years, gold(I) complexes have proven to be very efficient catalysts for activating C–C π bonds toward nucleophilic additions.[20−33] Accordingly, gold has been identified as an efficient hydroamination catalyst,[34−45] and a number of gold(I) complexes were found to work very efficiently with aryl and alkyl amines. However, hydroamination with small nucleophiles such as ammonia or hydrazine represents a much more challenging task.[46] In spite of the large interest for using these molecules in synthetic reactions, the examples available are yet rather scarce: Hartwig[47] and Buchwald[48] reported the palladium-catalyzed coupling of ammonia with aryl halides, whereas Stradiotto achieved the cross-coupling of aryl chlorides and tosylates with hydrazine.[49] One of the main difficulties that hamper the use of ammonia as N-nucleophile in transition-metal-catalyzed processes is the immediate formation of stable Werner ammine complexes, deactivating the catalyst.[46,50−53] In addition, the moderate basicity and low acidity of ammonia disfavor proton exchanges, either to or from ammonia.

The versatility and robustness of N-heterocyclic carbene ligands (NHC) have found wide application in gold catalysis,[54−56] and have allowed for the preparation of the first homogeneous catalyst active in the hydroamination with ammonia. Bertrand et al. reported gold(I) complexes with bulky cyclic (alkyl)(amino)carbene (**CAAC**) ligands[57−59] (Scheme 1) as efficient catalysts for the hydroamination of nonactivated multiple bonds with a variety of amines.[60−63] Moreover, they also discovered a CAAC–gold(I) complex as the first homogeneous catalyst active in the hydroamination of alkynes and allenes with ammonia.[64] Despite the fact that the gold(I)–CAAC species interacts with ammonia forming a Werner-type complex as the most stable initial intermediate, it

Scheme 1. Carbene–Gold(I) Catalysts for Hydrohydrazination of Alkynes Studied in the Present Work

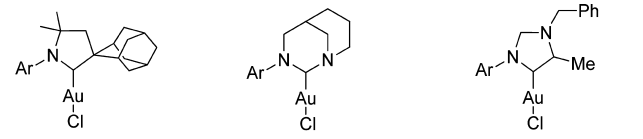

CAAC-Au complex **1-CAAC** | anti-Bredt-NHC-Au complex **1-antiB** | sa-NHC-Au complex **1-sa**

Ar = 2,6-diisopropylphenyl

Received: October 31, 2014
Revised: December 17, 2014
Published: December 18, 2014

DOI: 10.1021/cs501705b
ACS Catal. 2015, 5, 815–829

can catalyze the Markovnikov addition of NH_3 to C−C multiple bonds, yielding imines and allylamines.

The reactions with hydrazine involve various kinds of difficulties. First of all, similarly to ammonia, it readily forms very stable Werner complexes, which are generally inert for further reactions.[46,50−53] Moreover, hydrazine tends to act as a strong reductive agent,[65−67] which can easily lead to either the undesired formation of inactive metal particles[68,69] or the hydrogenation of unsaturated substrates.[70,71] These compounds can take place in metal-catalyzed N−N cleavage reactions leading to unwanted byproducts.[72−74] In order to avoid these undesired processes, up until recently the only possibility was using hydrazine derivatives, such as substituted hydrazines, hydrazones, or hydrazides;[75−82] however, these compounds do not represent an ideal solution when atom-efficiency is considered. Bertrand et al. demonstrated that cationic gold(I) complexes bearing a CAAC ligand also promoted the hydroamination of alkynes and allenes with parent hydrazine (Scheme 2),[83] although elevated temperatures (90−110 °C for alkynes and 130−150 °C for allenes) were required.

Scheme 2. Catalytic Hydroamination of Alkynes and Allenes with Hydrazine

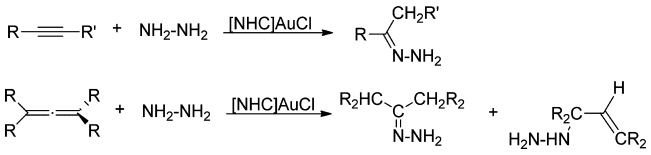

Subsequently, the same group showed that the reaction conditions can be improved by using NHC ligands in which one of the two nitrogen atoms of classical NHCs is placed in a strained bridgehead position (**anti-Bredt** NHC, Scheme 1).[84,85] In this way hydroamination of terminal alkynes with parent hydrazine at room temperature was achieved, and hydrazones were obtained.[86] Very recently, Hashmi et al. reported that gold(I) complexes with saturated abnormal NHC ligands (**sa** NHC, Scheme 1),[87,88] possessing only one nitrogen atom close to the carbene carbon atom, as CAAC and anti-Bredt NHC ligands, also catalyze the addition of hydrazine to terminal aryl and alkylalkynes at room temperature.[89] Moreover, the saNHC-Au(I) allows performing at room temperature the conversion of phenylacetylene into the corresponding hydrazone.

In the present work, we present the results of the theoretical investigations for the hydroamination of C−C multiple bonds of alkynes, alkenes, and allenes with hydrazine catalyzed by a series of gold(I)−carbene complexes experimentally reported. In order to get a complete picture of the factors affecting the efficiency of this synthetically relevant transformation, all the steps of the catalytic cycle have been computed using the three catalysts (Scheme 1) and several unsaturated substrates (Scheme 3).

MODELS AND COMPUTATIONAL METHODS

Calculations have been performed with the actual gold(I)−carbene complexes **1-CAAC**, **1-antiB** and **1-sa** (Scheme 1), without simplifications in the ligands. Alkynes (2-butyne **buty**, phenylacetylene **phacet** and benzylacetylene **bnacet**), as well as allenes (1,2-propadiene **prop** and tetraphenyl-1,2-propadiene **phprop**) and one alkene (2,3-dimethyl-2-butene **bute**) have been employed as substrates (Scheme 3). The solvent that gave

Scheme 3. Substrates for the NHC−Gold(I) Catalyzed Hydrohydrazination Studied in the Present Work

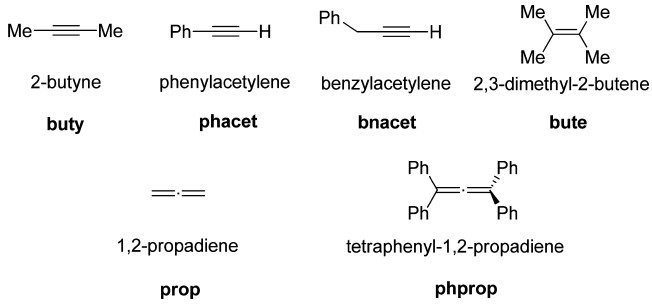

the optimum results in the experiments (benzene) has been considered in the theoretical study.

Calculations were performed at the DFT level using the M06 functional[90] including an ultrafine integration grid, as implemented in Gaussian 09.[91] Benchmark calibration studies to evaluate the performance of a number of density functionals on gold catalysis,[92] including hydroamination of ethyne by simple model complexes,[93] showed that M06 is one of the best-performing functionals both in terms of geometries and energies. The Au atom was described using the scalar-relativistic Stuttgart−Dresden SDD pseudopotential and its associated double-ζ basis set,[94] complemented with a set of f polarization functions.[95] The 6-31G(d,p) basis set was used for the H,[96] C, N, and Cl atoms.[97] The structures of the reactants, intermediates, transition states, and products were optimized in benzene solvent (ε = 2.2706), described by the SMD continuum model.[98] Frequency calculations were carried out for all the optimized geometries to characterize the stationary points as either minima or transition states. It was confirmed that transition states connect with the corresponding intermediates by means of application of the eigenvector corresponding to the imaginary frequency and subsequent optimization of the resulting structures. All the energies collected in the text are Gibbs energies in benzene at 298 K. Atomic charges were calculated using the Charge Model 5 (CM5). This population analysis approach gives charges essentially independent of the basis set.[99]

The structures are named according to the following procedure: ex. **TS_{Nuc}-CAAC-buty** where the first part describes the type of structure (a transition state), the second the ligand in the gold(I) complex (CAAC), and the third the unsaturated reactant.

RESULTS AND DISCUSSION

Mechanistic Considerations. Reaction mechanisms of gold-catalyzed processes have been the subject of intense debate.[100,101] Regarding the hydroamination reaction, there is agreement on the general reaction scheme. Commonly the reaction starts with the in situ generation of a catalytically active gold(I)−π complex[102,103] from a gold−chloride precursor. Subsequently, it involves nucleophilic attack of the N-nucleophile on a C−C π-bond, activated by coordination to the gold(I) center, and protodeauration of the alkenyl gold(I) intermediate. Despite this general agreement, aspects such as the associative or dissociative ligand exchange with the substrate, the generation of the catalytically active π-complex, the inner- or outer-sphere mechanism for the nucleophilic attack step, the nitrogen to carbon proton transfer or the relative importance of the ligand substitution, the nucleophilic

DOI: 10.1021/cs501705b
ACS Catal. 2015, 5, 815−829

addition and the proton transfer barriers in the catalytic cycle require deeper analysis, taking into account the nature of the ligands and the substrates. A recent paper has experimentally addressed ligand effects in the three major stages of gold-catalyzed reactions.[104] Ligand design in asymmetric gold catalysis using a combined experimental and theoretical approach has also been reported.[105] DFT studies have largely contributed to the general mechanistic perspective of gold(I)-catalyzed hydroamination,[106−110] providing information on the bonding aspects of intermediates, the proton shuttle role of the solvent, the counteranion or the N-nucleophile species itself in the protodeauration step, and the energetics of the full catalytic cycle. We first analyzed by means of theoretical methods the mechanism taking place in the hydroamination of alkynes with ammonia, catalyzed by Bertrand's gold−CAAC complex.[111] We established a plausible reaction mechanism (Scheme 4), which

Scheme 4. Proposed Catalytic Cycle for the Hydrohydrazination of Alkynes Catalyzed by NHC−Au(I) Complexes

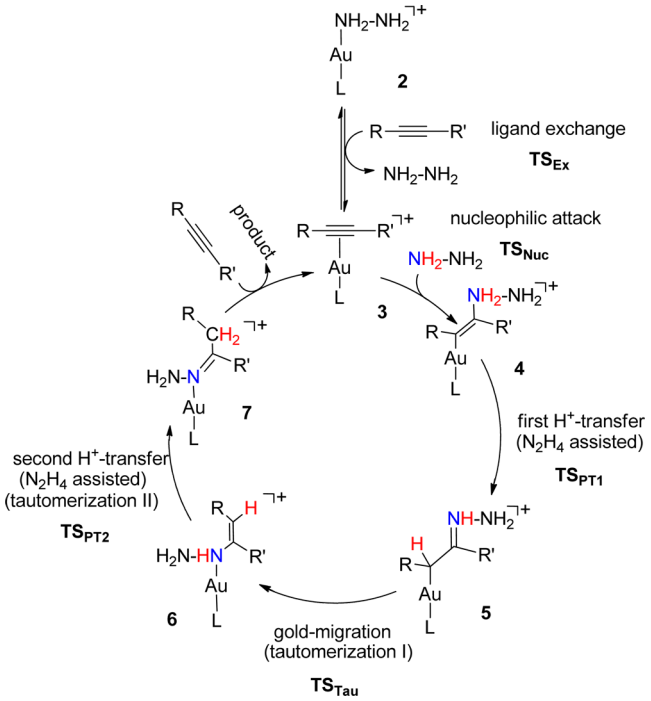

is consistent with kinetic experiments carried out by Bertrand et al.[64] In the case of hydrazine, the reaction mechanism explored follow the same general steps (Scheme 4; vide infra).

Calculations showed that, in spite of the fact that ammonia forms a strong complex with the gold center, Betrand's CAAC ligand does not prevent the formation of the alkyne π-complex, thus facilitating the reaction to take place by an outer-sphere nucleophilic attack. The formation of the C−N bond is followed by two subsequent proton transfer steps leading to the imine product. These steps involve tautomerization reactions, which are facilitated by the gold-center and the nucleophile molecules, present in excess in the solution under reaction conditions. In the present work, we have explored the feasibility of such mechanism (Scheme 4) for the hydrohydrazination of alkynes, alkenes, and allenes by Bertrand's and Hashmi's gold−carbene complexes, as detailed in the following sections.

Generation of the Active Species. According to the reaction mechanism described in Scheme 4, the active species has the substrate coordinated to the $[(NHC)Au]^+$ (**0**) moiety. This cationic fragment originates from the (carbene)gold chloride precursor (**1**) and an activator as tetrakis(3,5-bis(trifluoromethyl)phenyl)borate potassium salt, required for the halide abstraction.

$$[(NHC)AuCl] \rightarrow [(NHC)Au]^+ + Cl^- \quad (1)$$

The calculated ΔG in benzene for reaction 1 are 78.4, 78.1, and 82.0 kcal mol^{-1} for **1-CAAC**, **1-antiB** and **1-sa**, respectively. The high energy demand for removing the halide points out the compulsory use of a chloride abstractor. The charge analysis gives an estimation of the electrophilicity of the gold center in the (carbene)gold cations. The calculated charges are +0.16, +0.13, and +0.20 in **0-CAAC**, **0-antiB**, and **0-sa**, respectively. The charges are similar, though the sa carbene ligand gives a more positive gold atom. For the sake of comparison, we have calculated the charge of gold in the $[(PPh_3)Au]^+$ species; the lower value (+0.11) agrees with a more acidic gold center for the $[(NHC)Au]^+$ complexes here considered.[112]

The ΔG profiles in benzene for the generation of all the active π-complexes considered in the present work are presented in Figure 1.

Removing the Cl^- ligand from the (NHC)AuCl precatalyst opens a coordination site on the complex, which is filled by hydrazine. As expected, the most stable initial species are the Werner complexes. Hydrazine forms robust Werner complexes (**2**) with the $[(NHC)Au]^+$ fragments, with ΔG binding energies of 45.6, 45.4, and 48.0 kcal mol^{-1}, for **2-CAAC**, **2-antiB**, and **2-sa**, respectively. These complexes **2** are about 10 kcal mol^{-1} more stable than their counterparts with the substrate η^2-coordinated, **3**. Therefore, according to the general reaction mechanism (Scheme 4), the hydrazine Werner complexes can be considered the resting state of the catalysts. Complex **2-CAAC** was characterized by X-ray diffraction analysis.[83] The substitution reaction forming the active catalyst **3** takes place via an associative mechanism, through a transition state $\mathbf{TS_{Ex}}$ involving a tricoordinate gold center. The optimized structures of the hydrazine (**2-sa**) and phenylacetylene complexes (**3-sa-phacet**) as well as $\mathbf{TS_{Ex}}$**-sa-phacet** for the sa carbene ligand are depicted in Figure 2. All the alkynes present comparatively similar structures (Supporting Information).

In agreement with the endoergonic character of this ligand substitution, the transition state is product-like, with an elongated Au−N distance (2.57 Å) and N−Au−C_{sa} and C_{alkyne}−Au-C_{sa} angles of 128 and 154°. For alkynes, reaction barriers range from 10.0 kcal mol^{-1} ($\mathbf{TS_{Ex}}$**-sa-bnacet**)) to 14.4 kcal mol^{-1} ($\mathbf{TS_{Ex}}$**-antiB-bnacet** and $\mathbf{TS_{Ex}}$**-antiB-buty**) and follow the order of stability of the π-alkyne complexes. The $\Delta G^{\ddagger}_{Ex}$ are quite similar for a given substrate, the lower values corresponding to the **2-sa** complex. Hydrazine by alkene substitution has only been computed for the **2-sa** complex and 2,3-dimethyl-butene. The exchange barrier is slightly higher than that for 2-butyne (14.9 vs 12.1 kcal mol^{-1}). For the case of allenes, coordination is somehow more difficult, particularly when they bear bulky substituents ($\Delta G^{\ddagger}_{Ex}$ = 16.4 and 20.7 kcal mol^{-1} for 1,2-propadiene and tetraphenyl-1,2-propadiene, respectively). Comparing hydrazine to alkene and hydrazine to allene exchange, the exchange barrier is lower for the alkene. This result agrees with a higher stability of the alkene π-complex (Figure 1).

DOI: 10.1021/cs501705b
ACS Catal. 2015, 5, 815−829

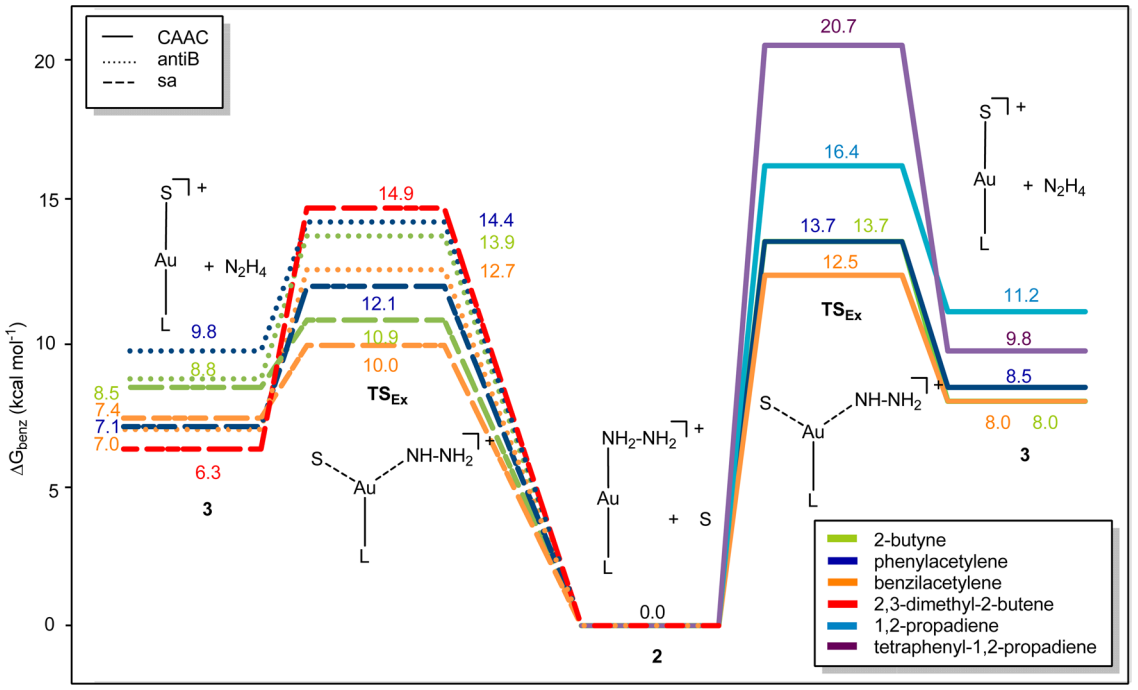

Figure 1. Generation of the active catalyst: Gibbs energy profiles (in benzene) for the substitution of hydrazine by all the substrates (S) for each of the considered NHC ligands (L). Right, L = CAAC; left L = antiB and sa.

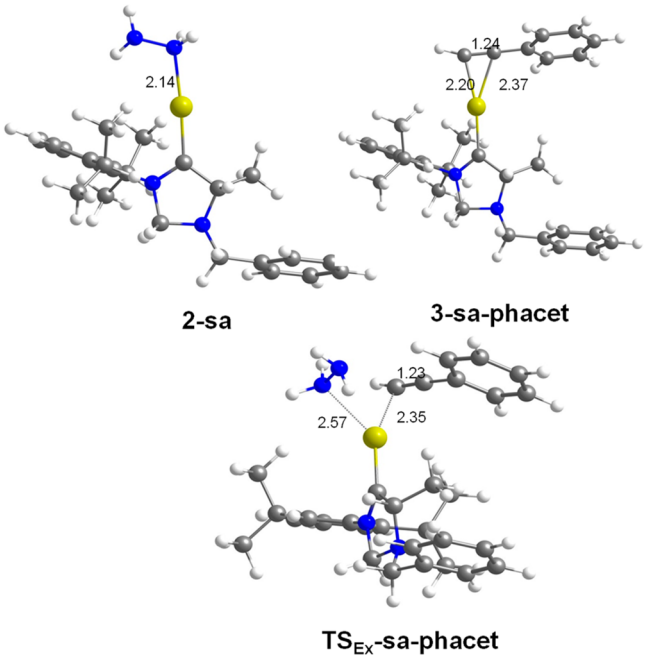

Figure 2. Optimized structures of the Werner complex **2-sa**, phenylacetylene π-complex **3-sa-phacet**, and the transition state for the ligand exchange, **TS_{Ex}-sa-phacet**.

Since the first isolation and structural characterization of cationic, two-coordinate gold π-arene complexes by Echavarren and co-workers[113] in 2006, a number of well-defined examples of two-coordinate, cationic π-complexes containing alkene, alkyne, and allene ligands have been documented.[114] The nature of the gold−substrate bond and the role of the ion-pair structure in solution have been investigated.[115] The gas-phase binding energies of unsaturated hydrocarbons (UHC) with the $[(PPh_3)Au]^+$ cation have been determined by means of mass spectrometry and DFT calculations.[116] The reported binding energies of phenylacetylene are 43.1 ± 0.9 kcal mol^{-1} (exptl) and 37.8 kcal mol^{-1} (calcd).[116] Our calculations, performed in benzene solvent, agree with a strong interaction between the $[(NHC)Au]^+$ and the unsaturated substrate: for phenylacetylene our calculated values are 38.4 ($[(CAAC)Au]^+$), 37.8 ($[(antiB)Au]^+$), and 37.8 ($[(sa)Au]^+$) kcal mol^{-1}. For each (carbene)gold−alkyne complex, the higher binding energy is found with benzylacetylene, though the differences caused by changing the unsaturated hydrocarbon ligand are small (less than 2 kcal mol^{-1}). The calculated binding energy is slightly higher for the $[(sa)Au(alkene)]^+$ complex (42.7 kcal mol^{-1}). As already noted, the binding affinity of alkenes relative to alkynes is strongly dependent on the alkene and alkyne substituents.[114,116] In this way, the calculated binding energies of allenes to $[(CAAC)Au]^+$ (ΔE in benzene) are 35.3 kcal mol^{-1} for 1,2-propadiene and 42.4 kcal mol^{-1} for tetraphenyl-1,2-propadiene. The calculated coordination Gibbs energies of 1,2-propadiene and tetraphenyl-1,2-propadiene to $[(CAAC)Au]^+$ are 21.5 and 23.0 kcal mol^{-1}, respectively. These values are substantially larger than that found for the coordination of (*S*)-penta-2,3-diene to a phosphine-gold cation, $[(PPh_3)Au]^+$, 9.2 kcal mol^{-1}.[107]

Coordination of the gold cation to terminal alkynes is not symmetrical. The distance between gold and the terminal carbon atom is around 0.15 Å shorter than the bond between the metal center and the internal carbon atom of the triple bond. The coordination of allenes to gold center has been a matter of intense investigations. In addition to the symmetric or "slipped" gold η^2-allene complexes, the presence of η^1-complexes, in which gold forms a bond with the central sp carbon atom of the allene, has also been proposed. The structures are very dependent on the nature of the allene substituents as well as on the properties of the particular gold complex employed.[117−120] The complex of $[(CAAC)Au]^+$ with both 1,2-propadiene (**3-prop**) and tetraphenyl-1,2-propadiene

DOI: 10.1021/cs501705b
ACS Catal. 2015, 5, 815−829

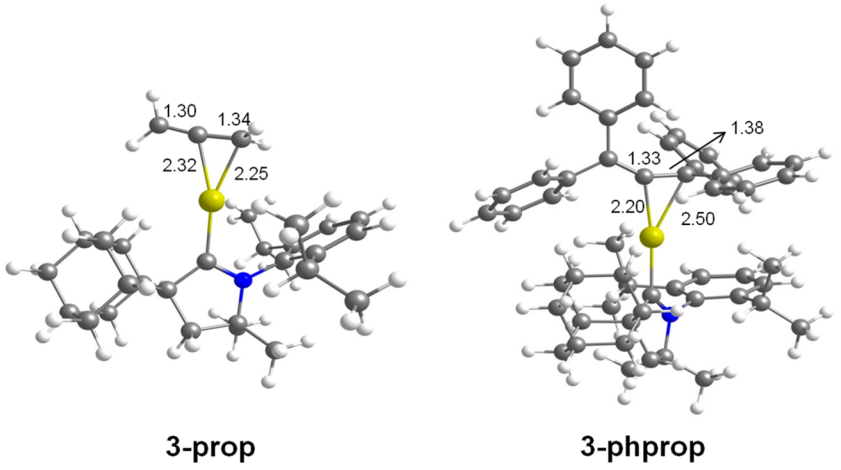

Figure 3. Optimized structures of the π-allene complexes with the [(CAAC)Au]$^+$ catalyst.

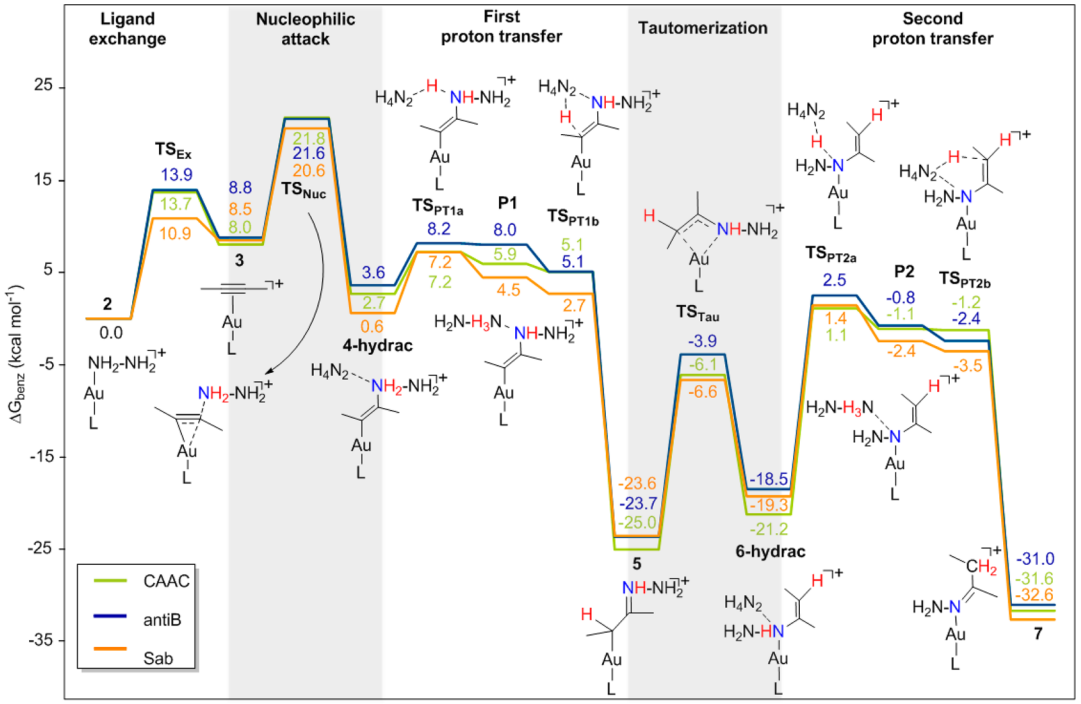

Figure 4. Gibbs energy profile in benzene for the hydrohydrazination of 2-butyne with the three [(NHC)Au]$^+$ catalysts considered.

(**3-phprop**) display a η^2-coordinate allene ligand. This is consistent with previous theoretical considerations:[117−120] for 1,2-propadiene the lack of substituents does not allow the stabilization of the η^1-complex, whereas for tetraphenyl-1,2-propadiene, the formation of such complex is sterically not favorable due to the presence of four bulky phenyl groups. The structure of the η^2-complexes (**3-prop** and **3-phprop**) is shown in Figure 3. The π-coordination is not completely symmetric. In **3-prop** the Au−C distance is somewhat longer for the central carbon atom than for the terminal one (d (Au−C) = 2.32 and 2.25 Å, respectively), while the opposite happens in **3-phprop** (d (Au−C) = 2.20 and 2.50 Å, respectively).

Coordination of the unsaturated hydrocarbon to the cationic [(NHC)Au]$^+$ entails its activation toward a nucleophilic attack by a net electron transfer from the UHC π-system to the electrophilic gold center. Natural Bond Analysis of the complexes displays that both ligand to metal donation and metal to ligand backdonation contribute to the gold−UHC interaction, as it has been recently pointed out.[103] The donation component is more important, leading to a positive charge on the ligand. The electron flow is similar in all the complexes (about 0.4 e), although for a particular alkyne, the highest value among the [(NHC)Au]$^+$ species is always found for the [(sa)Au]$^+$ complex. This is in agreement with the higher acidity of the gold atom in this cation. In the terminal alkynes, the positive charge is found on the internal carbon of the triple bond, in accordance with the Markovnikov-type addition reported.[83,86,89]

Overall, the study of the generation of the active species step shows that, despite [(CAAC)Au]$^+$, [(antiB)Au]$^+$, and [(sa)-Au]$^+$ forming strong Werner complexes with hydrazine, they also form strong complexes with unsaturated hydrocarbons, thus facilitating its replacement and the ulterior nucleophilic attack.

Hydroamination of Alkynes. The hydroamination of alkynes is presented in two sections. The first one describes the

DOI: 10.1021/cs501705b
ACS Catal. 2015, 5, 815−829

Table 1. Gibbs Energy of Activation for the Different Steps of the Hydrohydrazination and Overall Gibbs Energy of Reaction (ΔG_{reac}) and Gibbs Energy Barrier ($\Delta G^{\ddagger}_{act}$), in kcal mol^{-1}

	$\Delta G^{\ddagger}_{Ex}$	$\Delta G^{\ddagger}_{Nuc}$ [a]	$\Delta G^{\ddagger}_{PT1}$	$\Delta G^{\ddagger}_{Tau}$	$\Delta G^{\ddagger}_{PT2}$	$\Delta G^{\ddagger}_{act}$	ΔG_{reac}
2-butyne							
CAAC	13.7	13.8	4.5	18.9	22.3	26.1	−31.6
antiB	13.9	12.8	4.6	19.8	21.0	26.2	−31.0
sa	10.9	12.1	6.6	17.0	20.7	25.0	−32.6
phenylacetylene							
CAAC	13.7	7.7	0.6	21.0	19.1	23.2	−38.9
antiB	14.4	7.4	5.4	19.9	21.9	26.9	−38.8
sa	12.1	9.5	3.6	19.7	17.1	23.5	−40.0
benzylacetylene							
CAAC	12.5	9.4	1.4	22.6	20.9	29.0	−43.3
antiB	12.7	11.2	1.7	23.1	21.5	28.6	−44.0
sa	10.0	9.3	6.7	21.6	18.7	27.1	−41.0
2,3-dimethylbutene							
sa	14.9	18.1	36.5			52.0	−7.4
1,2-propadiene							
CAAC[b]	16.4	12.1	0.5	21.7	20.3	26.4	−43.4
CAAC[c]	16.4	11.5	10.3			22.7	−11.8
tetraphenyl-1,2-propadiene							
CAAC[b]	20.7	20.5	18.3	10.7	22.2	30.3	−21.1
CAAC[c]	20.7	11.5	9.6			29.1	+2.9

[a]From the π complexes 3. [b]Hydrazine addition at the central carbon atom. [c]Hydrazine addition at the terminal carbon atom.

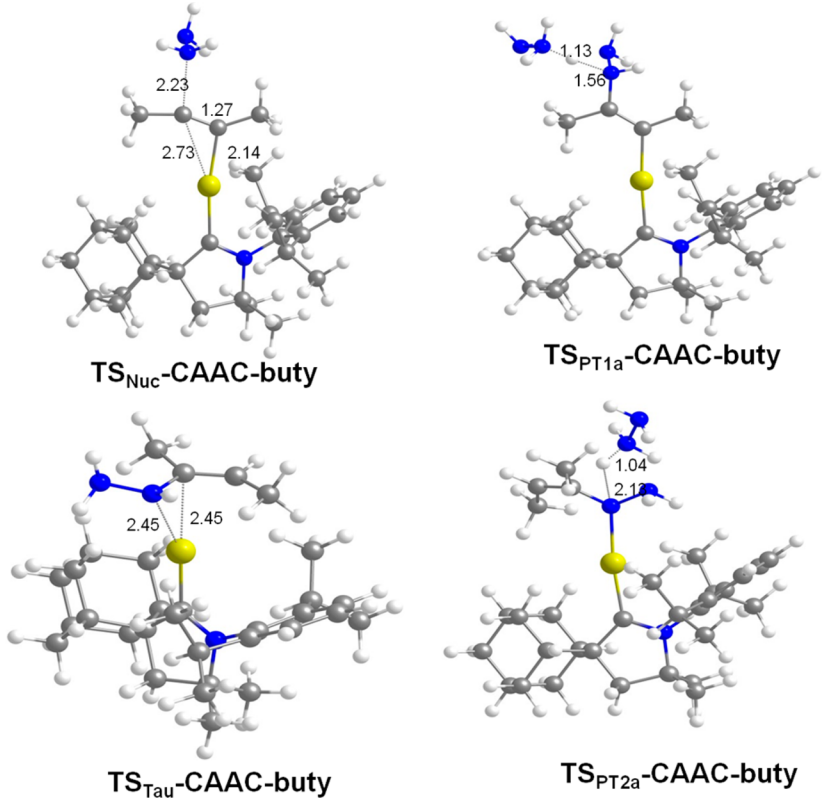

Figure 5. Transition states along the hydrohydrazination of 2-butyne catalyzed by [(CAAC)Au]$^{+}$.

process for an internal alkyne (2-butyne), whereas the second is devoted to terminal alkynes (phenyl- and benzylacetylene).

2-Butyne. We have chosen 2-butyne as an example of symmetrically substituted alkyne for the computational study. Hydroamination with hydrazine of internal alkynes has been only reported for diphenylacetylene. It takes place at 90−110 °C, yielding the corresponding hydrazone.[83,86]

As earlier mentioned, the mechanism of the hydroamination of alkynes with NH_3 using the [(CAAC)Au]$^{+}$ catalyst provides the basis for our analysis. After the hydrazine by alkyne ligand exchange, the reaction mechanism explored (Scheme 4) can be described in four main steps: (i) nucleophilic addition of hydrazine (ii), first proton transfer (assisted by the nucleophile), (iii) gold migration (tautomerization I) and (iv)

DOI: 10.1021/cs501705b
ACS Catal. 2015, 5, 815−829

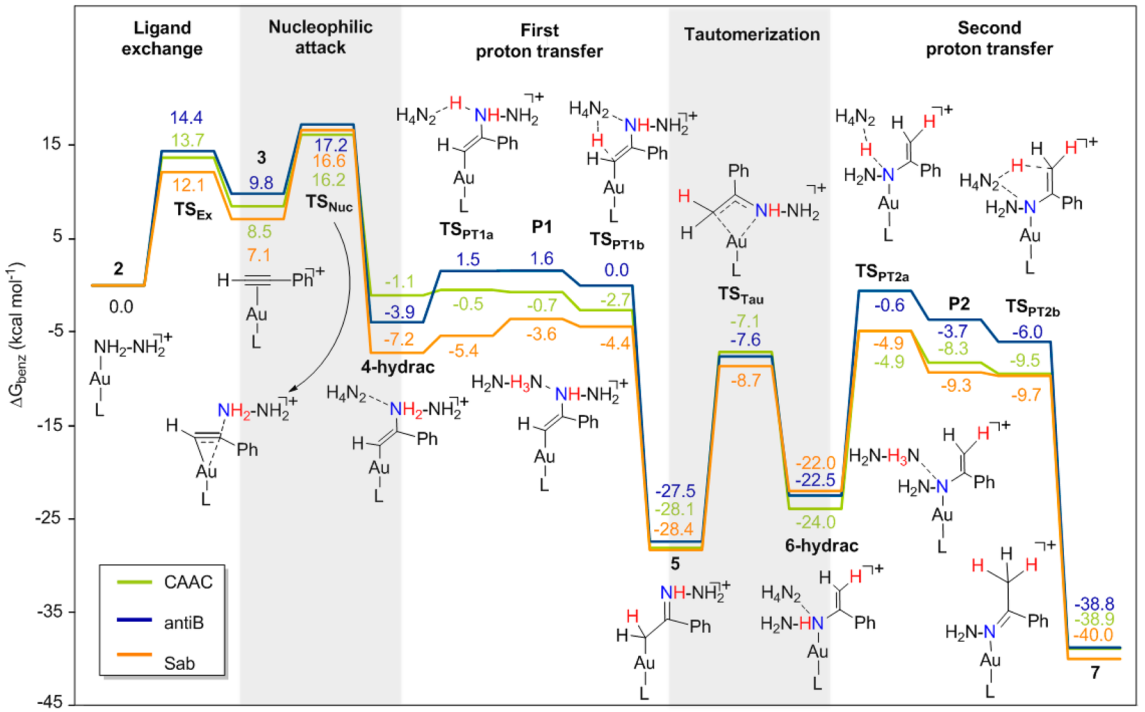

Figure 6. Gibbs energy profile in benzene for the hydrohydrazination of phenylacetylene with the three [(NHC)Au]$^+$ catalysts considered.

second proton transfer (also assisted by the nucleophile that can also be described as tautomerization II). The Gibbs energy profiles for the hydroamination of 2-butyne with the three gold(carbene) complexes are presented in Figure 4. The Gibbs energy of activation for each step ($\Delta G^{\ddagger}_{Ex}$, $\Delta G^{\ddagger}_{Nuc}$, $\Delta G^{\ddagger}_{PT1}$, $\Delta G^{\ddagger}_{Tau}$, and $\Delta G^{\ddagger}_{PT2}$) as well as the overall Gibbs activation energy ($\Delta G^{\ddagger}_{act}$ in the energetic span model)[121,122] and the Gibbs energy of reaction (ΔG_{reac}) of the full catalytic cycle are gathered in Table 1. Structures of the transition states for the [(CAAC)Au]$^+$ catalyst are collected in Figure 5. Very similar geometries are found in the case of all the three catalysts (see Supporting Information).

The inner or outer nature of the nucleophilic attack step in hydroamination reaction has been a matter of debate.[100,101] The detection of vinyl-gold complexes confirmed the prevalence of the outer sphere mechanism for the intramolecular gold-catalyzed hydroamination.[63,123] Very recently, Maier et al. has experimentally demonstrated that the same assumption also applies for the intermolecular version of the reaction.[124] Our calculated transition states for the nucleophilic attack of hydrazine agree with this picture (**TS$_{Nuc}$**, Figure 5).

N-deprotonation of the *trans*-alkenyl intermediates **4** formed by nucleophile addition leads to stable intermediates **5** with planar N atom and a C−C bond of single bond character, which can be described as protonated hydrazone. As it was found for the reaction with ammonia, one molecule of the nucleophile (hydrazine) is acting as a proton shuttle, taking a proton from the added hydrazine nitrogen to the alkenyl carbon. The first proton transfer takes place through two consecutive transition states (**TS$_{PT1a}$** and **TS$_{PT1b}$**), and an intermediate (**P1**) is obtained, which involves an [NH_2−NH_3]$^+$ moiety. Nevertheless, although two TS and one intermediate are found in the potential energy surface for the proton transfer, the three structures are very close in energy and only one transition state remains when thermal and entropic corrections are added (Gibbs energy profile, Figure 4). According to recent studies,[110,125,126] adventitious water molecules may play the same role of proton transfer agent than the nucleophile. The adventitious water-assisted proton transfer would most likely be a single-step sequence. A previous calculation of the water- and N-nucleophile-mediated (PhNH2) proton relay in a gold(I)-NHC promoted alkyne hydroamination provided similar activation barriers for both pathways.[110] From intermediate **5**, two subsequent tautomerization steps are required to obtain the final product. The first tautomerization is mediated by the gold-center: the gold-moiety migrates from the carbon to the nitrogen atom (**TS$_{Tau}$**, Figure 5) leading to the enamine-tautomer (**6**). Proton migration from the nitrogen to the carbon atom in **6** leads to the final hydrazone product **7.** The proton transfer in the enamine-tautomer takes place in two steps (**TS$_{PT2a}$** and **TS$_{PT2b}$**) through an intermediate with a $N_2H_5^+$-moiety (**P2**). Analogously to the first proton transfer, the Gibbs energy profile presents a single step for the second proton transfer (Figure 4).

There is a strong thermodynamic driving force for the hydroamination reaction: the hydrazone product (**7**) is more than 30 kcal mol^{-1} more stable than the reactants (Werner complex **2** plus the alkyne). The relative energy barriers for the nucleophilic attack, gold tautomerization and second proton transfer steps are similar (about 20 kcal mol^{-1}), whereas that for the first proton transfer is much lower (around 5 kcal mol^{-1}). According to the energy span model,[121,122] the activation energy of the full catalytic cycle is not determined by the nucleophilic attack step but by the difference between intermediate **5** (protonated hydrazone) and the transition state of the second proton transfer (**TS$_{PT2a}$**).[121,122] $\Delta G^{\ddagger}_{act}$ are practically equal for [(CAAC)Au]$^+$ and [(antiB)Au]$^+$ (26.1 and 26.2 kcal mol^{-1}, respectively), and is slightly lower for [(sa)Au]$^+$ (25.0 kcal mol^{-1}).[127]

Phenyl- and Benzylacetylene. Hydrohydrazination of phenylacetylene has been reported by Bertrand[86] using [(antiB)AuCl] (at 90 °C, 3h, 87% yield) and by Hashmi[89]

DOI: 10.1021/cs501705b
ACS Catal. 2015, 5, 815−829

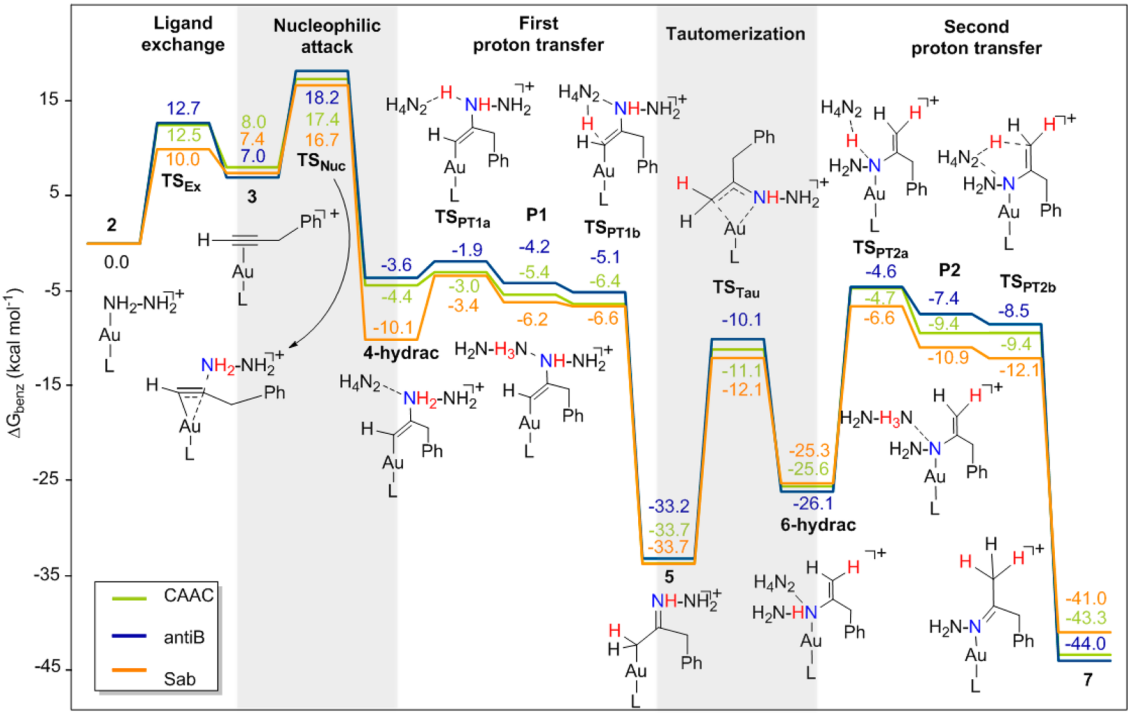

Figure 7. Gibbs energy profile in benzene for the hydrohydrazination of benzylacetylene with the three $[(NHC)Au]^+$ catalysts considered.

using [(sa)AuCl] (at 20 °C, 4 h, 90% yield). Hydrohydrazination of benzylacetlyne has been achieved with [(CAAC)AuCl] (at 100 °C, 3 h, 95% yield),[83] [(antiB)AuCl] (room temperature, 4 h, 83% yield)[86] and [(sa)AuCl] (room temperature, 4 h, 73% yield).[89] We have calculated the catalytic cycle for the hydroamination with hydrazine of both terminal alkynes using the three catalysts. The Gibbs energy profiles are displayed in Figures 6 (phenylacetlyene) and 7 (benzylacetylene). The Gibbs activation energies of each step are collected in Table 1.

The general appearance of the energy profiles for the phenylacetylene and benzylacetylene hydrohydrazination is similar to that for 2-butyne (Figure 4), although a close inspection reveals noticeable features. In agreement with the substituent effect expected for alkyl and aryl groups, the nucleophilic addition barriers for phenylacetylene (~16 kcal mol^{-1}) are lower than those for 2-butyne (~21 kcal mol^{-1}). Barriers for benzylacetylene are only around 1 kcal mol^{-1} higher than those for phenyl acetylene.

The nucleophilic addition step is easier with terminal alkynes than with internal ones. However, in both cases, the activation Gibbs energy of the hydroamination reaction is not governed by the nucleophilic addition step but by the energy difference between intermediates **5** (the protonated hydrazone) and the transition states of the second proton transfer ($\mathbf{TS_{PT2a}}$). The presence of a benzyl substituent substantially stabilizes intermediates **5**, without significantly modifying the energy of the transition step for the second proton transfer step ($\mathbf{TS_{PT2a}}$). Thus, $\Delta G^{\ddagger}_{act}$ for the hydrohydrazination of benzylacetylene are about 2.5 kcal higher than for 2-butyne with the same catalyst. Conversely, with phenylacetylene, intermediates **5** are found around 5 kcal mol^{-1} higher in energy than for benzylacetylene, thus decreasing $\Delta G^{\ddagger}_{act}$ about 5 kcal mol^{-1}. Overall, the $\Delta G^{\ddagger}_{act}$ calculated for phenylacetylene are the lowest ones. In the same way, hydroamination of the terminal alkynes is even more exergonic (~40 kcal mol^{-1}) than that of 2-butyne (~30 kcal mol^{-1}).

The relative stability of the intermediate formed after the first nitrogen to carbon proton migration (**5**) appears as an important factor in the Gibbs activation energy of the catalytic cycle. The other factor is the relative energy of the transition state corresponding to the deprotonation of the enamine intermediate (**6**). To assess the intrinsic acidity of the NH proton to be transferred in **6**, we have calculated the ΔG in benzene for the proton transfer reaction 3 involving the enamine (**6**):

$$[(NHC)Au(HNRNH_2)]^+ + N_2H_4 \rightarrow (NHC)Au(NRNH_2) + [N_2H_5]^+ \quad (3)$$

The $\Delta G^{\ddagger}_{PT2}$ correlates with this thermodynamic magnitude. Removal of the proton is about 5 kcal mol^{-1} more difficult for the 2-butyne intermediate than for the phenyl and benzyl alkynes, which exhibit similar ΔG values (about 30 kcal mol^{-1}). Comparing the action of the three catalysts, $[(sa)Au]^+$ is giving lower barriers than $[(antiB)Au]^+$ for both phenylacetylene and benzylacetylene substrates. This result agrees with the milder experimental conditions (room temperature) that are required for performing the hydrohydrazination of terminal alkynes with $[(sa)Au]^+$. However, the calculations do not reproduce the experimental trend found with the $[(antiB)Au]^+$ catalyst: hydroamination of benzylacetylene takes place at room temperature while 90 °C is required for the hydroamination of phenylacetylene. Conversely, the calculated barriers are 28.6 and 26.9 kcal mol^{-1}. Our calculated $\Delta G^{\ddagger}_{act}$ values for the hydroamination of benzylacetylene are always higher than those for phenylacetylene using the same catalyst. In addition to the accuracy of the computational methods for describing slight differences between overall energy barriers,[127] factors not considered in the calculations, as the instability of the $[(NHC)Au]^+$ complex, its deactivation by formation of catalytically inactive species[128] or the intervention of adventi-

DOI: 10.1021/cs501705b
ACS Catal. 2015, 5, 815−829

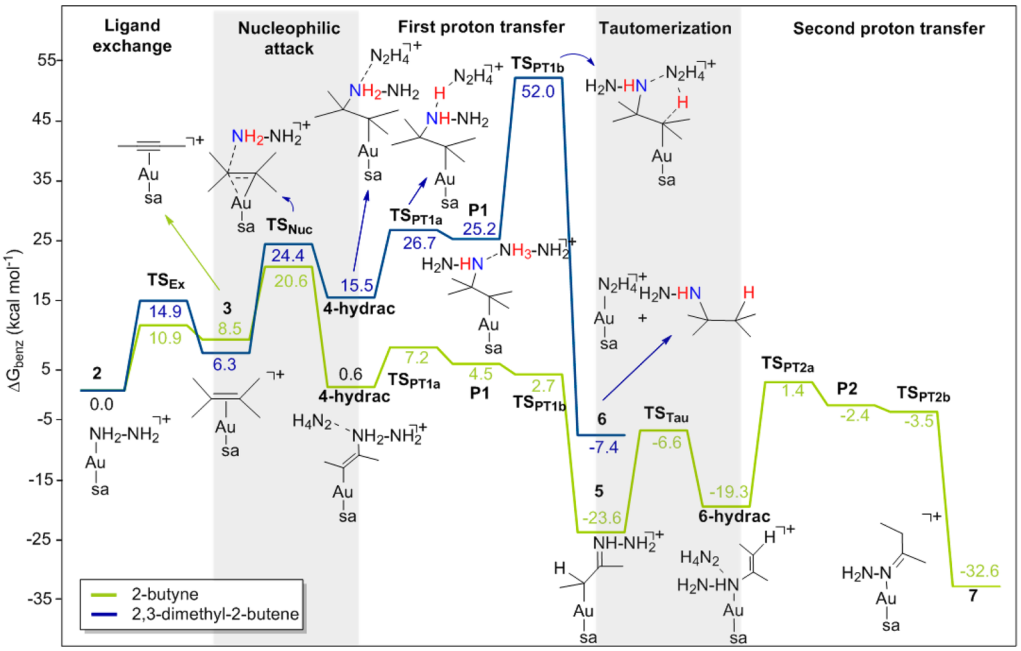

Figure 8. Comparison of the Gibbs energy profile in benzene for the hydrohydrazination of 2-butyne and 2,3-dimethyl-2-butene with the [(sa)Au]$^+$ catalyst.

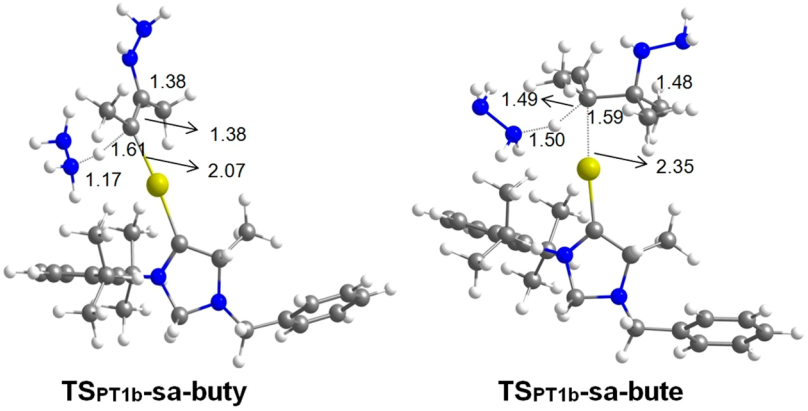

Figure 9. Optimized geometries of the transition states for the proton transfer to C atom of the C−C bond ($\mathbf{TS_{PT1b}}$) of 2,3-dimethyl-2-butene and 2-butyne, with the [(sa)Au]$^+$ catalyst.

tious water molecules in the proton transfer step,[110,125,126,129] may be at work. Calculations also foresee good efficiency of the [(CAAC)Au]$^+$ catalyst for the hydroamination of phenylacetylene, although no experimental results of this reaction have been reported.

Hydroamination of Alkenes. The intermolecular hydroamination of unactivated alkenes under mild conditions remains one of the most significant challenges in homogeneous catalysis. Activity of the three [(NHC)Au]$^+$ complexes studied in this work in the hydrohydrazination of alkenes has not been reported. However, for comparative purposes and also to identify the bottlenecks of this reaction, we have computationally studied the hydroamination of 2,3-dimethyl-2-butene with hydrazine, using [(sa)Au]$^+$ as catalyst. The obtained Gibbs energy profile is compared in Figure 8 with that of 2-butyne. As it can be appreciated in Figure 8, the barriers for the first two steps (hydrazine/π-substrate exchange and nucleophilic attack) are slightly higher for the alkene (about 4 kcal mol^{-1}), but still reachable. After the transition state of the nucleophilic attack ($\mathbf{TS_{Nuc}}$), the profiles diverge completely. Whereas for the alkyne the nucleophile attack process is practically ergoneutral (the adduct product lies only 0.6 kcal mol^{-1} above the initial state), for the alkene it lies 15.5 kcal mol^{-1} above the reactants.

The next step (N−H deprotonation) also entails a higher barrier for the alkene ($\mathbf{TS_{PT1a}}$), but the main discrepancy is found in the proton transfer to the carbon atom of the C−C bond ($\mathbf{TS_{PT1b}}$). With the alkyne this step leads, after crossing a low barrier, to very stable protonated hydrazone intermediates (**5**). For the alkene, this first protonation corresponds to the protodeauration step and already provides the final product (2-hydrazido-2,3-dimethylbutane) and the regeneration of the catalyst **2-sa**. Comparison of the structures of transition state $\mathbf{TS_{PT1b}}$ between the alkene and the alkyne systems (Figure 9) highlights the difficulties of protonating a sp^3 carbon atom, which entails the complete rupture of the Au−C bond.

Overall, the alkene hydroamination is exoergonic, although much less than with the alkyne (ΔG_{reac} are −7.4 and −32.6 kcal mol^{-1} for 2,3-dimethyl-2-butene and 2-butyne, respectively). However, a huge difference appears in the C-protonation barrier. The transition state for this reaction is found 52.0 kcal

DOI: 10.1021/cs501705b
ACS Catal. 2015, 5, 815−829

mol^{-1} above the reactants, completely preventing the hydrohydrazination of the alkene. Thus, the main difficulty to achieve alkene hydroamination is not related to the reactivity of the η^2-alkene gold(I) complex toward the nucleophilic attack but to the high barrier of the protodeauration step.

Hydroamination of Allenes. The gold-catalyzed addition of carbon-, oxygen- and nitrogen-based nucleophiles to allenes, leading to the formation of new C−O, C−N or C−C bonds, has emerged as an efficient strategy for the synthesis of natural products.[33] However, mechanistic studies of these reactions are scarce.[119,120] Toste and co-workers reported an intermolecular hydroamination reaction of allenes with hydrazide nucleophiles catalyzed by $[Ph_3PAu]^+$ and investigated the mechanism of this transformation. Their study suggested that the rate-determining transition state does not involve the nucleophile and that the active catalyst is monomeric in gold(I). Computational studies supported an outer-sphere mechanism.[107]

The reaction mechanism for the hydroamination of allenes with hydrazine, catalyzed by Bertrand's gold−CAAC complex is here analyzed by means of theoretical methods. For the analysis, we selected two concrete reactants studied by Bertrand et al.,[83] 1,2-propadiene (**prop**, **8**) and tetraphenyl-1,2-propadiene (**phprop**, **10**) (Scheme 5). Experimental results

Scheme 5. Catalytic Hydroamination Reactions of Allenes with Hydrazine Using 2-CAAC[83]

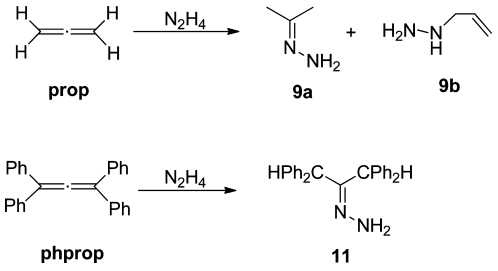

show that when the most simple allene, 1,2-propadiene, was treated with hydrazine in the presence of the gold-CAAC complex, a 2:1 mixture of hydrazone (**9a**) and allylhydrazine (**9b**) was obtained, whereas in the case of tetraphenyl-1,2-propadiene, only the hydrazone derivative (**11**) was observed (Scheme 5). The reaction takes place at higher temperatures than for alkynes (130 °C for 1,2-propadiene and 150 °C for tetraphenyl-1,2-propadiene).[83]

As reported for alkynes and alkenes, we have also characterized an outer-sphere attack of hydrazine on the π-coordinated allene active species **3**. However, the outer-sphere attack of hydrazine can take place on two different carbon atoms (the terminal or the central), leading to two different intermediates. With 1,2-propadiene, the transition state for the attack on the central carbon atom ($\mathbf{TS_{Nuc\text{-}cent}}$**-prop**) leads to complex **4-prop**, whereas the attack on the terminal carbon takes place via $\mathbf{TS_{Nuc\text{-}term}}$**-prop**, leading to **4′-prop** (Figure 10).

The Gibbs energy profile in benzene (Figure 11) reveals very similar barriers for both attacks, with the formed intermediates (**4-prop** and **4′-prop**) having also similar stability. The next step, a proton transfer, generates for both pathways much more stable intermediates (**5-prop** and **5′-prop**). For the pathway where the addition takes place on the terminal carbon, the reaction ends up after the first proton transfer at the allylhydrazine species (**5′-prop**), and subsequent decoordination generates the final product. For the attack on the internal carbon atom, the process takes place similarly to that for alkynes, leading to the hydrazone after gold migration from the carbon to the nitrogen and a second hydrazine assisted proton transfer from the nitrogen to the carbon. In this pathway, the activation energy of the full catalytic cycle is governed by the energy difference between intermediate **5-prop** and the transition state of the second proton transfer ($\mathbf{TS_{PT2}}$**-prop**). The global barrier ($\Delta G^{\ddagger}_{act}$ = 26.4 kcal mol^{-1}) is very close to that for the 2-butyne hydrohydrazination using the same catalyst (Table 1).

The selectivity is governed by the nucleophilic addition step. The experimentally observed regioselectivity (2:1 for **9a**:**9b**) would imply an energy difference between transition states of 0.4 kcal mol^{-1} favoring the internal addition. Computational results favor the external addition pathway by 0.6 kcal mol^{-1}. This energy difference lies within the error bars of the computational method, showing that these pathways are energetically quite close; the regioselectivity is thus quite subtle.

The reaction mechanism for the hydroamination of tetraphenyl-1,2-propadiene with hydrazine was also theoretically analyzed. For this allene, the reaction is regioselective and only one product (hydrazone), corresponding to the attack on the internal carbon, was experimentally observed (**11** in Scheme 4). We have computed the overall energy profiles for the hydrazine addition to both the internal and terminal carbon atoms (Figure 12). The reaction mechanism involves transition states and intermediates, which are in principle analogous to those obtained with 1,2-propadiene. Nevertheless, as far as the energy profiles are concerned they are quite different from those for 1,2-propadiene (Figure 11). These differences are responsible for the observed regioselectivity (vide infra).

The first step corresponds to the nucleophilic addition of hydrazine to the allene. For the addition to the allene central carbon atom, the transition state ($\mathbf{TS_{Nuc\text{-}cent}}$**-phprop**) is placed at a very similar energy than that for 1,2-propadiene (21.3 and 22.7 kcal/mol, respectively). However, the transition state for the nucleophilic attack on the terminal carbon atom is located considerably higher than that for 1,2-propadiene (30.3 and 23.3 kcal mol^{-1}, respectively). Both adducts **4-phprop** formed by hydrazine addition to the central and terminal carbons are significantly destabilized, compared with **4-prop**.

Major differences appear in the first proton transfer step. This step, which involves a low barrier with 1,2-propadiene, entails for the phenyl-substituted allene the highest energy transition state in the overall process. The global activation energy of the hydroamination process ($\Delta G^{\ddagger}_{act}$) is given by the energy difference between the resting state **2** and the transition state of the first proton transfer step ($\mathbf{TS_{PT1}}$**-phprop**). The $\Delta G^{\ddagger}_{act}$ values for tetraphenyl-1,2-propadiene (31.9 and 29.1 kcal mol^{-1}, Table 1) agree with the harsh conditions at which this reaction takes place (150 °C). The stability of the species **5-phprop** formed by protonation of the carbon atom is dramatically reduced with respect to the related **5-prop** complexes. Indeed, the formation of the allylhydrazine species becomes endoergonic by 2.9 kcal mol^{-1}.

The energy profiles in Figure 12 suggest that for tetraphenyl-1,2-propadiene, the reaction initiated by the nucleophilic addition to the terminal carbon atom is faster but reversible, whereas the nucleophilic addition to the central carbon atom is slower but irreversible. The energy barrier for the reverse reaction from the allylhydrazine complex **5-phprop** is only 26.2 kcal mol^{-1}. Overall, despite the fact that the addition on both

DOI: 10.1021/cs501705b
ACS Catal. 2015, 5, 815−829

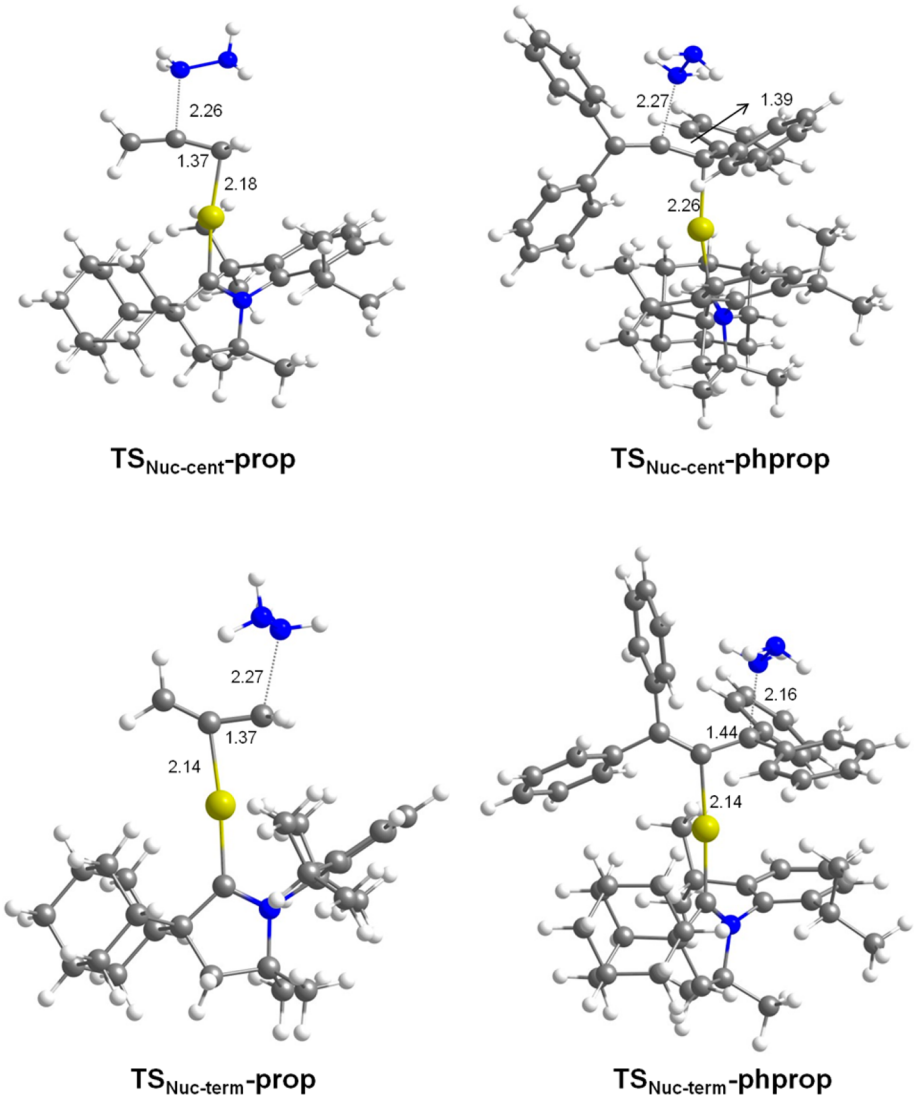

Figure 10. Optimized geometries for the possible outer-sphere nucleophile attacks of hydrazine on the η^2-allene complex with 1,2-propadiene and with tetraphenyl-1,2-propadiene, catalyzed by the $[(CACC)Au]^+$ complex.

the terminal and the central carbon atoms may take place, the latter gives rise to the experimentally observed product.

The mechanistic study with the two different substrates shows that for allenes the hydroamination reaction may take place through two different pathways (Scheme 6). They differ in the first step, the nucleophilic addition, which can take place at the central or at the terminal allene carbon atom. This step governs the regioselectivity of the process and, for the hydrazination, depending on the degree of substitution of the allene one or both pathways are taking place.

It is noteworthy that, in the intermolecular hydroamination of allenes, the nucleophile usually only adds to the terminal carbon atom of the allene.[29] Addition of Fmoc-protected ammonia[130] and aniline[131] yield only the corresponding allylamines. However, hydroamination with small nucleophiles, as ammonia and hydrazine, displays a different regioselectivity. Nucleophilic addition to 1,2-propadiene takes place on the terminal C with ammonia and both the terminal C and the central C with hydrazine. For the tetraphenylsubstituted allene addition of either ammonia or hydrazine only occurs on the central carbon atom. Our calculations agree with the existence of two competing pathways in which steric effect of both the allene and the nucleophile seems to influence the choice from the available options.

CONCLUSIONS

We investigated the reaction mechanism of the hydroamination of alkynes, alkenes and allenes with hydrazine catalyzed by the (carbene)gold(I) complexes experimentally reported by Bertrand's[83,86] and Hashmi's[89] groups. The general mechanism we reported for the reaction with ammonia[111] is also operating in the case of the hydrohydrazination of alkynes. This mechanism implies initial substitution of the hydrazine ligand in the Werner complex (resting state of the catalyst) by the unsaturated hydrocarbon, leading to a gold π-complex (catalytically active species). After the nucleophilic attack of hydrazine on the activated C−C bond, nitrogen to carbon atom proton transfer, assisted by the nucleophile, followed by carbon to nitrogen atom gold migration, yields the enamine intermediate. Then, a second nucleophile-assisted nitrogen to carbon atom proton transfer leads to the more stable imine tautomer. The $[(NHC)Au]^+$ species form strong Werner complexes with hydrazine, but they also form strong complexes with unsaturated hydrocarbons. The ligand substitution is

DOI: 10.1021/cs501705b
ACS Catal. 2015, 5, 815−829

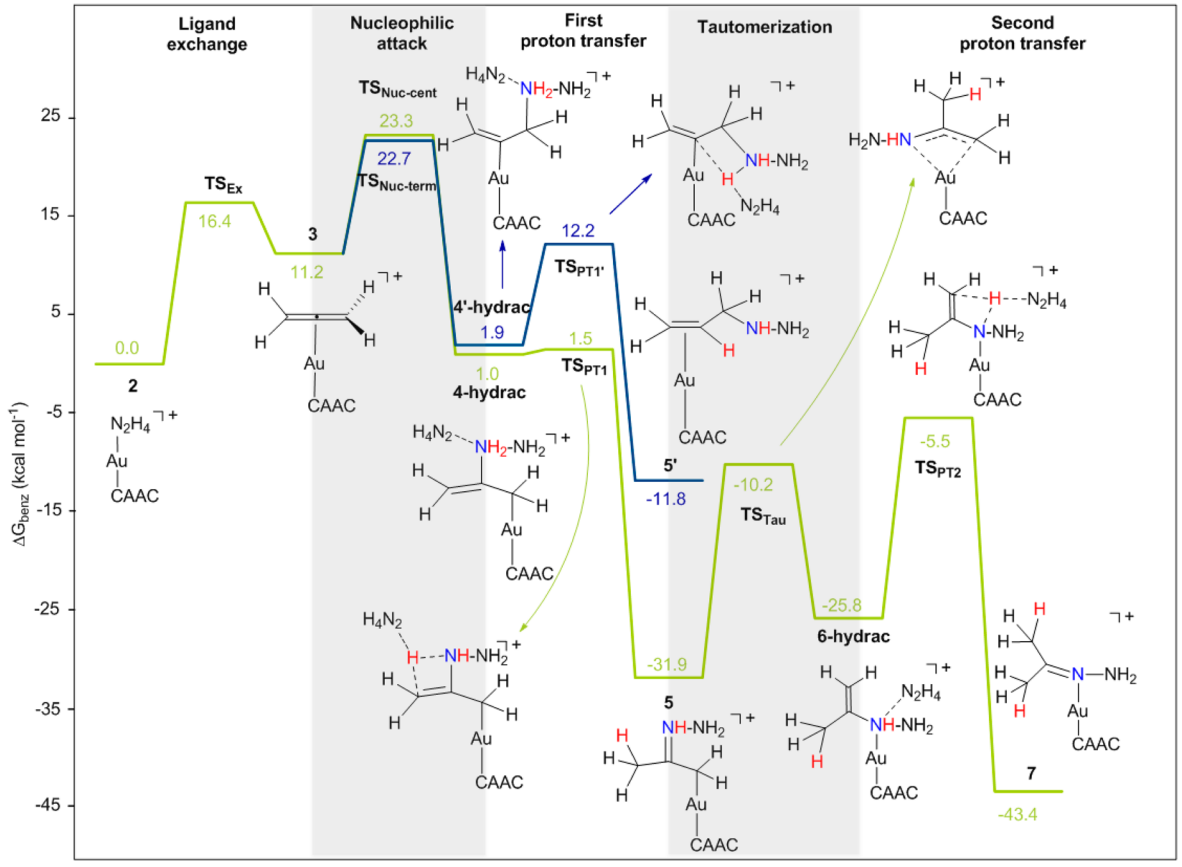

Figure 11. Gibbs energy profile in benzene for the hydroamination of 1,2-propadiene with hydrazine, catalyzed by [(CAAC)Au]$^+$. Green color: energy profile for the pathway leading to the major product (**9a**); blue color: energy pathway for the pathway leading to the minor product (**9b**).

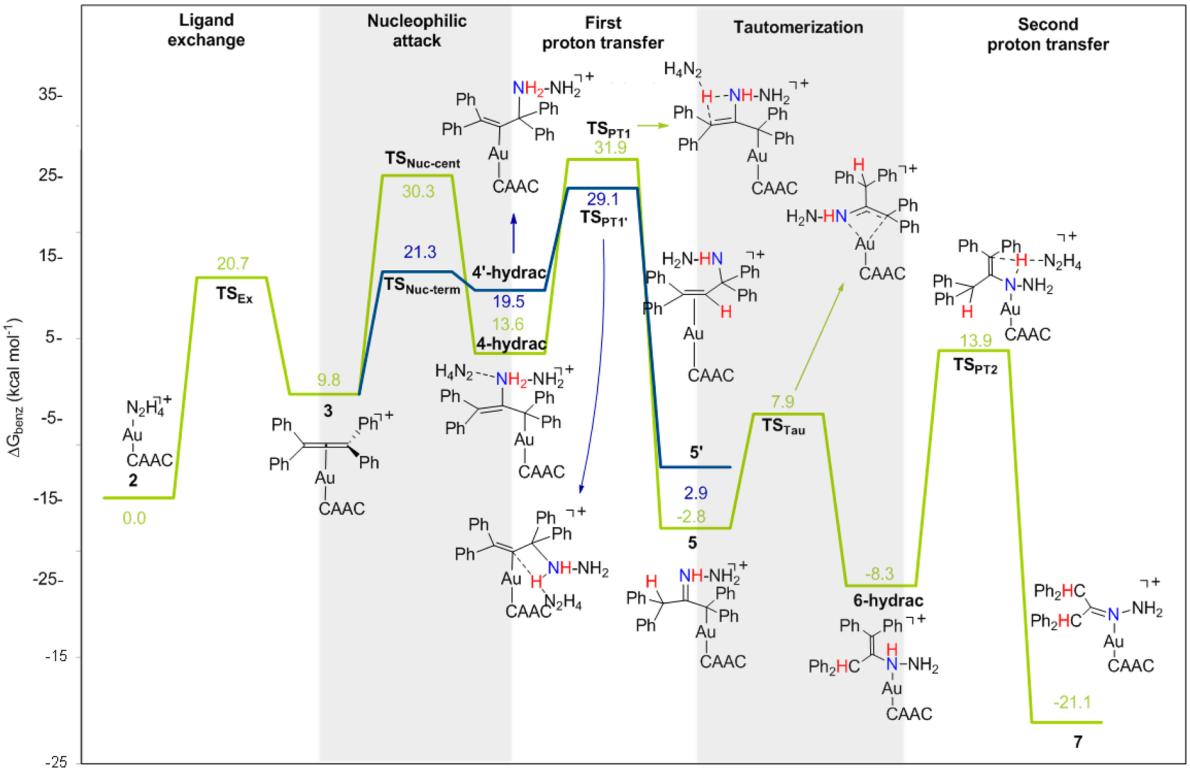

Figure 12. Gibbs energy profile in benzene for the hydroamination of tetraphenyl-1,2-propadiene with hydrazine, catalyzed by [(CAAC)Au]$^+$. Green color: energy profile for the terminal nucleophilic addition; blue color: energy pathway for the central nucleophilic addition.

DOI: 10.1021/cs501705b
ACS Catal. 2015, 5, 815−829

Scheme 6. Catalytic Cycle Proposed for the Hydroamination of Allenes with N_2H_4 Catalyzed by Bertrand's Gold−CAAC Complex

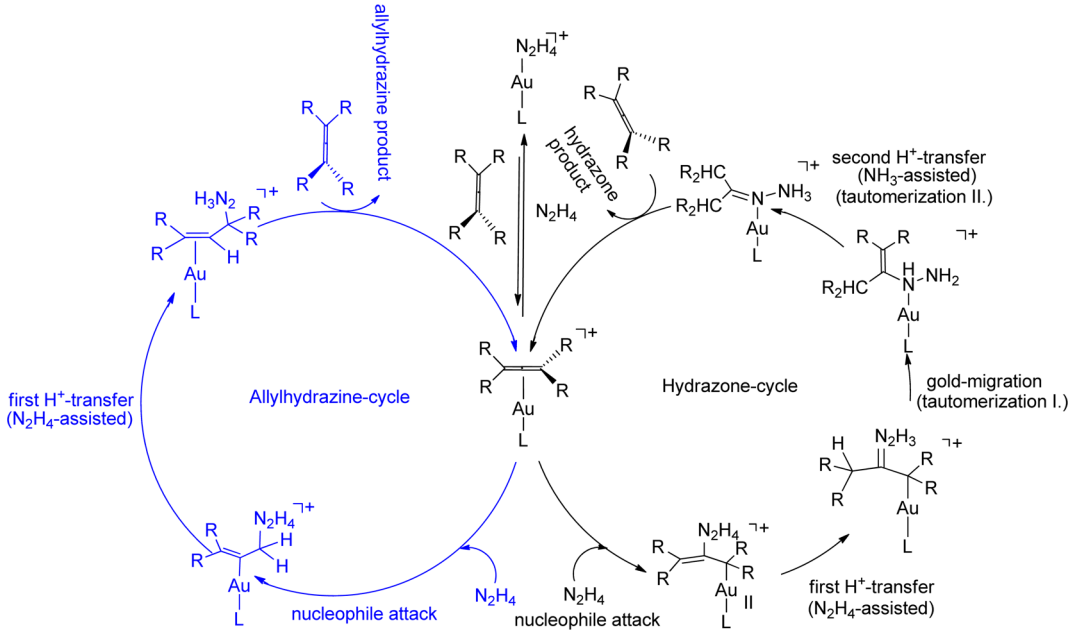

associative, takes place via tricoordinate transition states, and endergonic, but the energy barriers for this step with all the substrates analyzed make this ligand exchange feasible. Hydrazine by unsaturated hydrocarbon substitution can occur, provided that there is a thermodynamic driven force acting in the subsequent transformation of the π-complex.

Nucleophilic addition takes place via an outer sphere mechanism. For alkynes the energy barriers for the nucleophilic attack step follow the order 2-butyne > benzylacetylene > phenylacetylene. However, the activation energy of the full catalytic cycle, which ends up at the hydrazone, is not determined by the energy barrier of the nucleophilic attack but by the energy difference between the protonated hydrazone and the transition state of the second proton transfer. This energy difference follows the order benzylacetylene >2-butyne > phenylacetylene. Although the activation barriers are similar for the three gold−carbene complexes considered, they are slightly lower for $[(sa)Au]^+$, in agreement with the milder reaction conditions used with this catalyst. Concerning the hydrohydrazination of alkenes, our study points out that the main difficulty for this reaction is not the reactivity of the η^2-alkene gold(I) complex toward the nucleophilic attack but the protodeauration step. The high energy of the transition state of this step makes this reaction completely unfeasible.

We have found that the mechanism for the hydroamination of allenes with gold−carbene complexes is similar to that for the hydroamination of alkynes. In order to give an explanation for the different regioselectivity observed by Bertrand et al. in the hydroamination of 1,2-propadiene and tetraphenyl-1,2-propadiene,[83] we analyzed the pathways for the nucleophile attack on both the terminal and the internal carbon atoms of the η^2-allene complexes. Nucleophile attack on the internal carbon and subsequent proton transfer steps lead to the major product of the reaction in the 1,2-propadiene case and to the only product in the tetraphenyl-1,2-propadiene case, whereas the other attack and one subsequent proton transfer leads to the minor product in the case of 1,2-propadiene, and this product is not observed for the phenyl-substituted substrate. For 1,2-propadiene, the selectivity is governed by the nucleophilic addition step, which has very similar barriers for both attacks, allowing the obtaining of the mixture of hydrazone and allylhydrazine. For tetraphenyl-1,2-propadiene, the highest barrier corresponds to the first proton transfer. The reaction initiated by the nucleophilic addition to the terminal carbon atom is faster but reversible, whereas the nucleophilic addition to the central carbon atom is slower but irreversible. Therefore, only the latter product (hydrazone) is formed. Our calculations point out two competing pathways for the hydroamination of allenes. This result contrasts with the usual regioselectivity obtained in the intermolecular hydroamination of allenes, in which the nucleophile only adds to the terminal carbon atom of the allene, and highlights the role of both the substrate and the nucleophile in determining the reaction outcome.

We can conclude that herein we provide a comprehensive theoretical description of the hydroamination reaction of alkynes with a not very commonly used nucleophile, hydrazine, using (carbene)gold(I) complexes. By means of this work, we extended our theoretical analysis from ammonia to a similar but somewhat different nucleophile. Regarding the hydroamination of allenes, we showed how the proposed mechanism can account for regioselectivity. This study also reveals that the bottleneck for extending this reaction to alkenes is not the nucleophile attack but the proton transfer step. We think that the present study will serve as background for the design of further hydroamination reactions using simple small N-nucleophiles.

■ ASSOCIATED CONTENT

Supporting Information

The following file is available free of charge on the ACS Publications website at DOI: 10.1021/cs501705b.

Cartesian coordinates of the optimized structures, absolute energies, and Gibbs energies in benzene (Hartrees) of all the calculated species (PDF)

DOI: 10.1021/cs501705b
ACS Catal. 2015, 5, 815−829

AUTHOR INFORMATION

Corresponding Authors

*E-mail: agusti@klingon.uab.es.
*E-mail: gregori@klingon.uab.es.

Notes

The authors declare no competing financial interest.

ACKNOWLEDGMENTS

Financial support from the Spanish Ministerio de Economia y Competitividad (project CTQ2014-54071-P) and by the CMST COST Action CM1205 "Catalytic Routines for Small Molecule Activation" (CARISMA) is gratefully acknowledged. A.C.-R. is grateful to the Spanish MINECO for a FPI Fellowship.

REFERENCES

(1) Hong, S.; Marks, T. J. *Acc. Chem. Res.* **2004**, *37*, 673−686.
(2) Severin, R.; Doye, S. *Chem. Soc. Rev.* **2007**, *36*, 1407−1420.
(3) Patil, N. T.; Yamamoto, Y. *Chem. Rev.* **2008**, *108*, 3395−3442.
(4) Muller, T. E.; Hultzsch, K. C.; Yus, M.; Foubelo, F.; Tada, M. *Chem. Rev.* **2008**, *108*, 3795−3892.
(5) Fukumuto, Y. *J. Synth. Org. Chem. Jpn.* **2009**, *67*, 735−750.
(6) Patil, N. T.; Kavthe, R. D.; Shinde, V. S. *Tetrahedron* **2012**, *68*, 8079−8146.
(7) Hesp, K. D.; Stradiotto, M. *ChemCatChem.* **2010**, *2*, 1192−1207.
(8) Hannedouche, J.; Schulz, E. *Chem.—Eur. J.* **2013**, *19*, 4972−4985.
(9) Nishina, N.; Yamamoto, Y. *Topics Organometallic Chem.* **2013**, *43*, 115−143.
(10) Kawatsura, M.; Hartwig, J. F. *J. Am. Chem. Soc.* **2000**, *122*, 9546−9547.
(11) Stahl, S. S. *Angew. Chem., Int. Ed.* **2004**, *43*, 3400−3420.
(12) Phua, P. H.; Mathew, S. P.; White, A. J. P.; de Vries, J. G.; Blackmond, D. G.; Hii, K. K. *Chem.—Eur. J.* **2007**, *13*, 4602−4613.
(13) Ahmed, M.; Seayad, A. M.; Jackstell, R.; Beller, M. *Angew. Chem., Int. Ed.* **2003**, *42*, 5615−5619.
(14) Utsunomiya, M.; Kuwano, R.; Kawatsura, M.; Hartwig, J. F. *J. Am. Chem. Soc.* **2003**, *125*, 5608−5609.
(15) Field, L. D.; Messerle, B. A.; Voung, K. Q.; Turner, P. *Organometallics* **2005**, *24*, 4241−4250.
(16) Oe, Y.; Ohta, T.; Ito, Y. *Chem. Commun.* **2004**, 1620−1621.
(17) Utsunomiya, M.; Hartwig, J. F. *J. Am. Chem. Soc.* **2004**, *126*, 2702−2703.
(18) Quian, H.; Han, X.; Widenhoefer, R. A. *J. Am. Chem. Soc.* **2004**, *126*, 9536−9537.
(19) Toups, K. L.; Widenhoefer, R. A. *Chem. Commun.* **2010**, *46*, 1712−1714.
(20) Jimenez-Nuñez, E.; Echavarren, A. M. *Chem. Commun.* **2007**, 333−346.
(21) Hashmi, A. S. K. *Chem. Rev.* **2007**, *107*, 3180−3211.
(22) Fürstner, A.; Davies, P. W. *Angew. Chem., Int. Ed.* **2007**, *46*, 3410−3449.
(23) Widenhoefer, R. A. *Chem.—Eur. J.* **2008**, *14*, 5382−5391.
(24) Li, Z.; Brouwer, C.; He, C. *Chem. Rev.* **2008**, *108*, 3239−3265.
(25) Arcadi, A. *Chem. Rev.* **2008**, *108*, 3266−3325.
(26) Jiménez-Nuñez, E.; Echavarren, A. M. *Chem. Rev.* **2008**, *108*, 3326−3350.
(27) Gorin, D. J.; Sherry, B. D.; Toste, F. D. *Chem. Rev.* **2008**, *108*, 3351−3378.
(28) Fürstner, A. *Chem. Soc. Rev.* **2009**, *38*, 3208−3221.
(29) Hashmi, A. S. K.; Bührle, M. *Aldrichimica Acta* **2010**, *43*, 27−33.
(30) Shapiro, N. D.; Toste, F. D. *Synlett* **2010**, 675−691.
(31) Huang, H.; Zhou, Y.; Liu, H. *Beilstein J. Org. Chem.* **2011**, *7*, 897−936.
(32) Corma, A.; Leyva-Perez, A.; Sabater, M. J. *Chem. Rev.* **2011**, *111*, 1657−1712.
(33) Krause, N.; Winter, C. *Chem. Rev.* **2011**, *111*, 1994−2009.
(34) Widenhoefer, R. A.; Han, X. *Eur. J. Org. Chem.* **2006**, 4555−4563.
(35) Zhang, J.; Yang, C.-G.; He, C. *J. Am. Chem. Soc.* **2006**, *128*, 1798−1799.
(36) Zhang, Z. B.; Bender, C. F.; Widenhoefer, R. A. *J. Am. Chem. Soc.* **2007**, *129*, 14148−14149.
(37) Leseurre, L.; Toullec, P. Y.; Genet, J. P.; Michelet, V. *Org. Lett.* **2007**, *9*, 4049−4052.
(38) Giner, X.; Nájera, C. *Org. Lett.* **2008**, *10*, 2919−2922.
(39) Enomoto, T.; Obika, S.; Yasui, Y.; Takemoto, Y. *Synlett.* **2008**, *11*, 1647−1650.
(40) Zhang, X.; Corma, A. *Dalton Trans.* **2008**, *3*, 397−403.
(41) Yeh, M. C. P.; Pai, H. F.; Lin, Z. J.; Lee, B. R. *Tetrahedron* **2009**, *65*, 4789−4794.
(42) Patil, N. T.; Kavthe, R. D.; Raut, V. S.; Shinde, V. S.; Balasubramanian, S. *J. Org. Chem.* **2010**, *75*, 1277−1280.
(43) Li, H.; Lee, S. D.; Widenhoefer, R. A. *J. Org. Chem.* **2011**, *696*, 316−320.
(44) Butler, K. L.; Tragni, M.; Widenhoefer, R. A. *Angew. Chem., Int. Ed.* **2012**, *51*, 5175−5178.
(45) Michon, C.; Abadie, M.-A.; Medina, F.; Agbossou-Niedercorn, F. *Catal. Today* **2014**, *235*, 2−13.
(46) Klinkenberg, J. L.; Hartwig, J. F. *Angew. Chem., Int. Ed.* **2011**, *50*, 86−95.
(47) Shen, Q.; Hartwig, J. F. *J. Am. Chem. Soc.* **2006**, *128*, 10028−10029.
(48) Surry, D. S.; Buchwald, S. L. *J. Am. Chem. Soc.* **2007**, *129*, 10354−10355.
(49) Lundgren, R. J.; Stradiotto, M. *Angew. Chem., Int. Ed.* **2010**, *49*, 8686−8690.
(50) Heaton, B. T.; Jacob, C.; Page, P. *Coord. Chem. Rev.* **1996**, *154*, 193−229.
(51) van der Vlugt, J. I. *Chem. Soc. Rev.* **2010**, *39*, 2302−2322.
(52) Young, P. C.; Green, S. L. J.; Rosair, G.; Lee, A.-L. *Dalton Trans.* **2013**, *42*, 9645−9653.
(53) Kim, J.; Kim, H. J.; Chang, S. *Eur. J. Org. Chem.* **2013**, 3201−3213.
(54) Marion, N.; Nolan, S. P. *Chem. Soc. Rev.* **2008**, *37*, 1776−1782.
(55) Nolan, S. P. *Acc. Chem. Res.* **2011**, *44*, 91−100.
(56) Kumar, A.; Ghosh, P. *Eur. J. Inorg. Chem.* **2012**, 3955−3969.
(57) Lavallo, V.; Canac, Y.; Präsang, C.; Donnadieu, B.; Bertrand, G. *Angew. Chem., Int. Ed.* **2005**, *44*, 5705−5709.
(58) Lavallo, V.; Canac, Y.; DeHope, A.; Donnadieu, B.; Bertrand, G. *Angew. Chem., Int. Ed.* **2005**, *44*, 7236−7239.
(59) Jazzar, R.; Dewhurst, R. D.; Bourg, J. B.; Donnadieu, B.; Canac, Y.; Bertrand, G. *Angew. Chem., Int. Ed.* **2007**, *46*, 2899−2902.
(60) Zeng, X.; Solelilhavoup, M.; Bertrand, G. *Org. Lett.* **2009**, *11*, 3166−3169.
(61) Xeng, X.; Frey, G. D.; Kousar, S.; Bertrand, G. *Chem.—Eur. J.* **2009**, *15*, 3056−3060.
(62) Zeng, X.; Frey, G. D.; Kinjo, R.; Donnadieu, B.; Bertrand, G. *J. Am. Chem. Soc.* **2009**, *131*, 8690−8696.
(63) Zeng, X.; Kinjo, R.; Donnadieu, B.; Bertrand, G. *Angew. Chem., Int. Ed.* **2010**, *49*, 942−945.
(64) Lavallo, V.; Frey, G. D.; Donnadieu, B.; Soleilhavoup, M.; Bertrand, G. *Angew. Chem., Int. Ed.* **2008**, *47*, 5224−5228.
(65) Greenwood, N. N.; Earnshaw, A. *Chemistry of the Elements*; Elsevier: Oxford, 1998; pp 427−431.
(66) Roden, B. A. Hydrazine. In *Encyclopedia of Reagents for Organic Synthesis*; Paquette, L. A., Ed.; Wiley: Chichester, U.K., 2001.
(67) Celier, P. P.; Spindler, J. F.; Taillefer, M.; Cristau, H. J. *Tetrahedron Lett.* **2003**, *44*, 7191−7195.
(68) Simpson, D. K. *Met. Finish.* **1985**, *83*, 57−60.
(69) Chen, J. P.; Lim, L. L. *Chemosphere* **2002**, *49*, 363−370.
(70) Smit, C.; Fraaije, M. W.; Minnaard, A. J. *J. Org. Chem.* **2008**, *73*, 9482−9485.
(71) Dhakshinammorthy, A.; Alvaro, M.; Garcia, H. *Adv. Synth. Catal.* **2009**, *351*, 2271−2276.

DOI: 10.1021/cs501705b
ACS Catal. 2015, 5, 815−829

(72) Alonso, F.; Radivoy, G.; Yus, M. *Tetrahedron* **2000**, *56*, 8673−8678.
(73) Ellames, G. J.; Gibson, J. S.; Herbert, J. M.; McNeill, A. H. *Tetrahedron* **2001**, *57*, 9487−9497.
(74) Lee, K.-S.; Lim, Y.-K.; Cho, C.-G. *Tetrahedron Lett.* **2002**, *43*, 7463−7464.
(75) Mizushima, E.; Hayashi, T.; Tanaka, M. *Org. Lett.* **2003**, *5*, 3349−3352.
(76) Li, Y.; Shi, Y.; Odom, A. L. *J. Am. Chem. Soc.* **2004**, *126*, 1794−1803.
(77) Patil, N. T.; Lutete, L. M.; Nishina, N.; Yamamoto, Y. *Tetrahedron Lett.* **2006**, *47*, 4749−4751.
(78) Johns, A. M.; Liu, Z.; Hartwig, J. F. *Angew. Chem., Int. Ed.* **2007**, *46*, 7259−7261.
(79) Dabb, S. L.; Messerle, B. A. *Dalton Trans.* **2008**, 6368−6371.
(80) Halland, N.; Nazaré, M.; Alonso, J.; R'kyek, O.; Lindenschmidt, A. *Chem. Commun.* **2010**, *47*, 1042−1044.
(81) Kramer, S.; Madsen, J. L. H.; Rottländer, M.; Skrydsrup, T. *Org. Lett.* **2010**, *12*, 2758−2761.
(82) LaLonde, R. L.; Wang, Z. J.; Mba, M.; Lackner, A. D.; Toste, F. D. *Angew. Chem., Int. Ed.* **2010**, *49*, 598−601.
(83) Kinjo, R.; Donnadieu, B.; Bertrand, G. *Angew. Chem., Int. Ed.* **2011**, *50*, 5560−5563.
(84) Martin, D.; Lassauque, N.; Donnadieu, B.; Bertrand, G. *Angew. Chem., Int. Ed.* **2012**, *51*, 6172−6175.
(85) Martin, D.; Lassauque, N.; Steinmann, F.; Manuel, G.; Bertrand, G. *Chem.—Eur. J.* **2013**, *19*, 14895−14901.
(86) López-Gómez, M. J.; Martin, D.; Bertrand, G. *Chem. Commun.* **2013**, *49*, 4483−4485.
(87) Hashmi, A. S. K.; Riedel, D.; Rudolph, M.; Rominger, F.; Oeser, T. *Chem.—Eur. J.* **2012**, *18*, 3827−3830.
(88) Manzano, R.; Rominger, F.; Hashmi, A. S. K. *Organometallics* **2013**, *32*, 2199−22203.
(89) Manzano, R.; Wurm, T.; Rominger, F.; Hashmi, A. S. K. *Chem.—Eur. J.* **2014**, *20*, 6844−6848.
(90) Zhao, Y.; Truhlar, D. *Theor. Chem. Acc.* **2008**, *120*, 215−241.
(91) Frisch, M. J.; Trucks, G. W.; Schlegel, H. B.; Scuseria, G. E.; Robb, M. A.; Cheeseman, J. R.; Scalmani, G.; Barone, V.; Mennucci, B.; Petersson, G. A.; Nakatsuji, H.; Caricato, M.; Li, X.; Hratchian, H. P.; Izmaylov, A. F.; Bloino, J.; Zheng, G.; Sonnenberg, J. L.; Hada, M.; Ehara, M.; Toyota, K.; Fukuda, R.; Hasegawa, J.; Ishida, M.; Nakajima, T.; Honda, Y.; Kitao, O.; Nakai, H.; Vreven, T.; Montgomery, J. A., Jr.; Peralta, J. E.; Ogliaro, F.; Bearpark, M.; Heyd, J. J.; Brothers, E.; Kudin, K. N.; Staroverov, V. N.; Kobayashi, R.; Normand, J.; Raghavachari, K.; Rendell, A.; Burant, J. C.; Iyengar, S. S.; Tomasi, J.; Cossi, M.; Rega, N.; Millam, M. J.; Klene, M.; Knox, J. E.; Cross, J. B.; Bakken, V.; Adamo, C.; Jaramillo, J.; Gomperts, R.; Stratmann, R. E.; Yazyev, O.; Austin, A. J.; Cammi, R.; Pomelli, C.; Ochterski, J. W.; Martin, R. L.; Morokuma, K.; Zakrzewski, V. G.; Voth, G. A.; Salvador, P.; Dannenberg, J. J.; Dapprich, S.; Daniels, A. D.; Farkas, Ö.; Foresman, J. B.; Ortiz, J. V.; Cioslowski, J.; Fox, D. J. *Gaussian 09*, revision D.01; Gaussian, Inc.: Wallingford CT, 2009.
(92) Nieto Faza, O.; Álvarez Rodríguez, R.; Silva López, C. *Theor. Chem. Acc.* **2011**, *128*, 647−661.
(93) Ciancaleoni, G.; Rampino, S.; Zuccaccia, D.; Tarantelli, F.; Belanzoni, P.; Belpassi, L. *J. Chem. Theory Comput.* **2014**, *10*, 1021−1034.
(94) Andrae, D.; Haeussermann, U.; Dolg, M.; Stoll, H.; Preuss, H. *Theor. Chim. Acta* **1990**, *77*, 123−141.
(95) Ehlers, A. W.; Bohme, M.; Dapprich, M. S.; Gobbi, A.; Hollwarth, A.; Jonas, V.; Kohler, K. F.; Stegmann, R.; Veldkamp, A.; Frenking, G. *Chem. Phys. Lett.* **1993**, *208*, 111−114.
(96) Hehre, W. J.; Ditchfield, R.; Pople, J. A. *J. Chem. Phys.* **1972**, *56*, 2257−2261.
(97) Francl, M. M.; Pietro, W. J.; Hehre, W. J.; Binkley, J. S.; Gordon, M. S.; DeFrees, D. J.; Pople, J. A. *J. Chem. Phys.* **1982**, *77*, 3654−3665.
(98) Marenich, A. V.; Cramer, C. J.; Truhlar, D. G. *J. Phys. Chem. B* **2009**, *113*, 6378−6396.
(99) Marenich, A. V.; Jerome, S. V.; Cramer, C. J.; Truhlar, D. G. *J. Chem. TheoryComput.* **2012**, *8*, 527−54.
(100) Hashmi, A. S. K. *Angew. Chem., Int. Ed.* **2010**, *49*, 5232−5241.
(101) Obradors, C.; Echavarren, A. M. *Chem. Commun.* **2014**, *50*, 16−28.
(102) Brooner, R. E. M.; Widenhoefer, R. A. *Angew. Chem., Int. Ed.* **2013**, *52*, 11714−11724.
(103) Zuccaccia, D.; Belpassi, L.; Macchioni, A.; Tarantelli, F. *Eur. J. Inorg. Chem.* **2013**, 4121−4135.
(104) Wang, W.; Hammnond, G. B.; Xu, B. *J. Am. Chem. Soc.* **2012**, *134*, 5697−5705.
(105) Teller, H.; Corbet, M.; Mantilli, L.; Gopakumar, G.; Goddard, R.; Thiel, W.; Fürstner, A. *J. Am. Chem. Soc.* **2012**, *134*, 15331−15342.
(106) Kovács, K.; Ujaque, G.; Lledós, A. *J. Am. Chem. Soc.* **2008**, *130*, 853−864.
(107) Wang, Z. J.; Benitez, D.; Tkatchouk, E.; Goddard, W. A., III; Toste, F. D. *J. Am. Chem. Soc.* **2010**, *132*, 13064−13071.
(108) Giner, X.; Nájera, C.; Kovács, G.; LLedós, A.; Ujaque, G. *Adv. Synth. Catal.* **2011**, *353*, 3451−3466.
(109) Kim, J. H.; Park, S.-W.; Park, S. R.; Lee, S.; Kang, E. J. *Chem.—Asian J.* **2011**, *6*, 1982−1986.
(110) Katari, M.; Rao, M. N.; Rajaraman, G.; Ghosh, P. *Inorg. Chem.* **2012**, *51*, 5593−5604.
(111) Kovács, G.; Lledós, A.; Ujaque, G. *Angew. Chem., Int. Ed.* **2011**, *50*, 11147−11151.
(112) Charges calculated with other schemes, as Hirshfeld and Natural Population Analysis, give the same ordering for the charges on gold atom in this series of compounds.
(113) Herrero-Gómez, E.; Nieto-Oberhuber, C.; López, S.; Benet-Buchholz, J.; Echavarren, A. M. *Angew. Chem., Int. Ed.* **2006**, *45*, 5455−5459.
(114) Brooner, R. E M.; Widenhoefer, R. A. *Angew. Chem., Int. Ed.* **2013**, *52*, 11714−11724.
(115) Zuccaccia, D.; Belpassi, L.; Macchioni, A.; Tarantelli, F. *Eur. J. Inorg. Chem.* **2013**, 4121−4135.
(116) Jasiková, L.; Roithová, J. *Organometallics* **2012**, *31*, 1935−1942.
(117) Gandon, V.; Lemière, G.; Hours, A.; Fensterbank, L.; Malacria, M. *Angew. Chem., Int. Ed.* **2008**, *47*, 7534−7538.
(118) Montserrat, S.; Ujaque, G.; López, F.; Mascareñas, J. L.; Lledós, A. *Top. Curr. Chem.* **2011**, *302*, 225−248.
(119) Yang, W.; Hashmi, A. S. K. *Chem. Soc. Rev.* **2014**, *43*, 2941−2955.
(120) Soriano, E.; Fernández, E. *Chem. Soc. Rev.* **2014**, *43*, 3041−3105.
(121) Kozuch, S.; Shaik, S. *Acc. Chem. Res.* **2011**, *44*, 101−110.
(122) Kozuch, S. *WIREs Comput. Mol. Sci.* **2012**, *2*, 795−815.
(123) Hashmi, A. S. K.; Ramamurthi, T. D.; Rominer, F. *Adv. Synth. Catal.* **2010**, *352*, 971−975.
(124) Zhdanko, A.; Maier, M. E. *Angew. Chem., Int. Ed.* **2014**, *53*, 7760−7764.
(125) Krauter, C. M.; Hashmi, A. S. K.; Pernpointner, M. *ChemCatChem.* **2010**, *2*, 1226−1230.
(126) Kovács, G.; Lledós, A.; Ujaque, G. *Organometallics* **2010**, *29*, 3252−3260.
(127) A simple calculation, using the transition state theory, gives a 298 K a five-times increase in the reaction rate for 1 kcal mol^{-1} decrease in the $\Delta G^{\ddagger}_{act}$.
(128) Kumar, M.; Jasinski, J.; Hammond, G. B.; Xu, B. *Chem.—Eur. J.* **2014**, *20*, 3113−3119.
(129) The stabilized hydrazine monohydrate was employed in the reaction with the $[(sa)Au]^+$ catalyst (ref 89). There is evidence that adventitious water molecules can participate as proton shuttle in proton transfer steps (refs 110, 125, and 126).
(130) Kinder, R. E.; Zhang, Z.; Widenhoefer, R. A. *Org. Lett.* **2008**, *10*, 3157−3159.
(131) Nishina, N.; Yaamamoto, Y. *Angew. Chem., Int. Ed.* **2006**, *45*, 3314−3317.

DOI: 10.1021/cs501705b
ACS Catal. 2015, 5, 815−829